Developmental Regulation of p66^{Shc} Is Altered by Bronchopulmonary Dysplasia in Baboons and Humans

Matt K. Lee, Gloria S. Pryhuber, Margaret A. Schwarz, Susan M. Smith, Zdena Pavlova, and Mary E. Sunday

Center for Craniofacial Molecular Biology, School of Dentistry, University of Southern California, and the Neonatology Division, Departments of Pediatrics and Pathology, University of Southern California/Los Angeles County Medical Center, Los Angeles, California; Department of Pediatrics, Golisano Children's Hospital at Strong, University of Rochester Medical Center, Rochester, New York; Robert Wood Johnson Medical School, University of Medicine and Dentistry of New Jersey, New Brunswick, New Jersey; and Department of Pathology, Brigham and Women's Hospital, Harvard Medical School, Boston, Massachusetts

Rationale: **The p66^{Shc} adapter protein antagonizes mitogen-activated protein, or MAP, kinase, mediates oxidative stress, and is developmentally regulated in fetal mouse lungs.** ***Objectives:*** **To determine if p66^{Shc} is similarly regulated in primates and in bronchopulmonary dysplasia (BPD), which results from oxidative injury to immature lungs.** ***Methods:*** **Normal and injured lungs from humans and baboons were evaluated by Western analysis and immunohistochemistry.** ***Measurements and Main Results:*** **In baboons, p66^{Shc} decreased 80% between 125 and 175 days' gestation ($p = 0.025$), then doubled after term delivery at 185 days ($p = 0.0013$). In the hyperoxic 140-day fetal baboon BPD model, p66^{Shc} expression persisted, and its localization shifted from the epithelium of gestational controls to the mesenchyme of diseased lungs, coincident with expression of proliferating cell nuclear antigen and cleaved poly(adenyl ribose) polymerase, a marker of apoptosis. Treatment with the anti-bombesin antibody 2A11 attenuated BPD, reduced cell proliferation, increased p66^{Shc} expression 10.5-fold, and preserved epithelial p66^{Shc} localization. p66^{Shc} also decreased during normal human lung development, falling 87% between 18 and 24 weeks' gestation ($p = 0.02$). p66^{Shc} was expressed throughout 18-week human lungs, became restricted to scattered epithelial cells by 24 weeks, and localized to isolated mesenchymal cells after term delivery. In contrast, p66^{Shc} remained prominent in the epithelium of lungs with acute injury or mild BPD, and in the mesenchyme of lungs with severe disease. p66^{Shc} localized to tissues expressing proliferating cell nuclear antigen and cleaved poly(adenyl ribose) polymerase.** ***Conclusions:*** **p66^{Shc} expression, cell proliferation, and apoptosis are concomitantly altered during lung development and in BPD.**

Keywords: fetal development; lung; MAP kinases; ShcA protein

Lung development is regulated by interactions between epithelial and mesenchymal cells. These interactions are typically mediated by growth factors that bind cognate receptors to initiate intracellular phosphorylation cascades. The developmental expression of these factors controls important aspects of lung morphogenesis. However, signaling components within targeted cells may also be developmentally regulated. Growth factor receptors typically phosphorylate adaptor proteins that combine with other proteins to activate downstream effectors. Important examples include the Shc protein family, which comprises three isoforms with different functions. On tyrosine phosphorylation, the ubiquitous 52-kD isoform (p52^{Shc}) complexes with Grb2 and Sos and translocates to the plasma membrane where it encounters and activates Ras, thus initiating the mitogen-activated protein (MAP) kinase cascade, culminating in cell proliferation (1). A 46-kD alternative translation product appears to function similarly (2). Although Shc is a canonic substrate of tyrosine kinase receptors, such as that of epidermal growth (3) factor and insulin (4), it is also associated with signaling by G-protein–coupled receptors (5) and integrins (6).

A third isoform of 66 kD (p66^{Shc}) results from an alternative splice reaction that appends 109 amino acids to p52^{Shc}. Unlike the other isoforms, p66^{Shc} antagonizes Ras activation (2) and mediates oxidative stress–induced apoptosis (7). We have reported that, although p52^{Shc} is highly expressed at all stages of fetal mouse lung development, p66^{Shc} is highly expressed only through the 18th day of gestation, after which its expression decreases precipitously (8). This expression pattern may be of particular interest in the preterm human lung, which is uniquely exposed to wide fluctuations in oxidative stress loads and highly susceptible to bronchopulmonary dysplasia (BPD), a chronic disease of the immature lung. Moreover, p66^{Shc} primarily localizes to mesenchymal cells adjoining the basement membranes of large and intermediate airways within the fetal mouse lung. Mesenchymal cell proliferation is characteristic of severe BPD. We therefore hypothesized that p66^{Shc} is developmentally regulated in normal fetal human and baboon lungs, and that this regulation is distorted by the pathogenesis of BPD.

Two animal models of BPD were evaluated. The original characterization of BPD (9) emphasized areas of atelectasis interspersed with regions of compensatory emphysema, interstitial fibrosis, epithelial metaplasia, and chronic reactive airways disease with peribronchial smooth muscle hypertrophy. This severely fibrotic BPD was reproduced using baboons delivered at 140 days' gestation and maintained in 100% oxygen (10), and is attenuated by intravenous infusion of antibodies against bombesin-like peptides (BLPs) (11). With advances in neonatal therapy, the clinical presentation of BPD has evolved and is currently characterized by reduced interstitial fibrosis, chronic reactive airways disease, and attenuated alveolar septation within more premature lungs (12). This mildly fibrotic form of BPD was modeled using baboons delivered at 125 days' gestation and benefiting from lower oxygen concentrations, intrauterine corticosteroids, and exogenous surfactant. Our results in both animal models and in postmortem human specimens suggest that p66^{Shc} expression in the primate lung is developmentally regulated in isoform-specific fashion, and that the normal ontogeny of Shc isoform expression is disrupted by the onset of BPD. Some of the results of these studies have been previously reported in the form of an abstract (13).

(*Received in original form June 18, 2004; accepted in final form March 15, 2005*)

Supported by National Institutes of Health grants NIH R01 HL02929 (M. K. L. and S. M. S.), NIH R01 HL63039 (G. S. P.), R01 HL52638 (M.E.S.), resource grant HL-52636, and NIH R-10 Collaborative Program in Bronchopulmonary Dysplasia, directed by Dr. Jacqueline Coalson.

Correspondence and requests for reprints should be addressed to Matt Lee, M.D., USC CCMB, 2250 Alcazar Street, CSA-113, Los Angeles, CA 90033. E-mail: mattlee@usc.edu

This article has an online supplement, which is accessible from this issue's table of contents at www.atsjournals.org

Am J Respir Crit Care Med Vol 171. pp 1384–1394, 2005
Originally Published in Press as DOI: 10.1164/rccm.200406-776OC on March 18, 2005
Internet address: www.atsjournals.org

TABLE 1. CLINICAL HISTORIES ASSOCIATED WITH AUTOPSY SPECIMENS

Case ID	Sex	Birth Weight (*g*)	Gest Age at Birth (*wk*)	Postnatal Age at Death (*d*)	Gest Age at Death (*wk*)	Autopsy Diagnosis	$FiO_2 > 50\%$ (*d*)	On IMV (*d*)
No lung disease								
Case 1	F	2,580	36	2	36	Hypoxic-ischemic encephalopathy	2	2
Case 2	F	1,880	36	4	37	Severe microcephaly	2	4
Case 3	F	2,035	40	5	41	Pena-Shokeir phenotype	0	1
BPD								
Case 4	M	825	27	97	40	BPD, periventricular leukomalacia	96	97
Case 5	F	910	26	60	35	BPD, brain infarct	23	32
Case 6	M	520	25	65	34	BPD, cytomegalovirus infection, hypertropic cardiomyopathy	30	62
Case 7	M	1,021	28	13	30	BPD, intrauterine growth retardation, cytomegalovirus	13	13
Sepsis								
Case 8	F	620	25	18	27	Necrotizing enterocolitis, pulmonary hemorrhage, BPD	7	18
Case 9	M	1,037	27	1	27	Acute chorioamnionitis with funisitis	1	1
Case 10	F	1,210	28	32	33	Fulminate necrotizing enterocolitis	3	3
Case 11	M	1,940	31	5	32	*E. coli* sepsis	5	4

Definition of abbreviations: BPD = bronchopulmonary dysplasia; Gest = gestational; IMV = intermittent mandatory ventilation.

METHODS

Normal Baboon Tissues

Fetal baboon tissue was provided by the Southwest Foundation for Biomedical Research under protocols approved by the Animal Care Committee of that institution. The National Research Council Guide for the Care and Use of Laboratory Animals was strictly adhered to. Normal lungs were obtained at 125, 140, 160, and 175 days' gestation. At least four fetuses were analyzed for each time point. Four specimens were obtained 1, 2, and 3 days after term delivery at 185 days and pooled as the postpartum cohort.

Baboon BPD Models

Mildly fibrotic BPD was induced in baboons delivered at 125 days' gestation and treated with intrauterine betamethasone, exogenous surfactant, endotracheal intubation, minimal respiratory support required to maintain arterial carbon dioxide between 45 and 55 mm Hg, and minimal oxygen necessary to maintain arterial oxygen between 55 and 70 mm Hg (14). Severely fibrotic BPD was induced in animals delivered at 140 days and exposed to 10 days of 100% oxygen (15). BPD in this model is attenuated by adsorbing circulating BLPs. Animals received intravenous infusions of either anti-BLP antibody (2A11) or nonspecific control antibody (MOPC-21; Sigma, St. Louis, MO) (11). Histologic specimens were fixed in 4% paraformaldehyde. For Western analysis, left-lower-lobe lung sections were snap-frozen in liquid nitrogen. At least four animals were analyzed for each experimental condition.

Human Tissues

Human tissues were obtained under protocols approved by the Institutional Review Boards of Advanced Bioscience Resources, Strong Memorial Hospital, and the University of Southern California/Los Angeles County Medical Center. Snap-frozen lung tissues from 12 normal fetuses were provided by Advanced Bioscience Resources (Alameda, CA). Pathologic specimens represent 12 infants who died in the intensive care nursery of Strong Memorial Hospital (Rochester, NY). Clinical synopses are provided in Table 1. Patients were clinically diagnosed with BPD based on delivery before 32 weeks' gestation, intubation for neonatal respiratory distress syndrome, and mechanical ventilation with supplemental oxygen for at least 13 days. Pathologic diagnoses of BPD were based on epithelial metaplasia, mesenchymal thickening, and alveolar dysplasia. Specimens were also obtained from infants succumbing to nonpulmonary disorders and whose autopsies indicated normal lung histology. Samples were processed within 6 hours of death.

Western Analysis

Western analyses were performed as described (8) using an anti-Shc antibody (Transduction Laboratories, Lexington, KY). Samples were equalized by total protein and equivalent loading confirmed by glyceraldehyde phosphate dehydrogenase (Chemicon, Temecula, CA) reprobe and/or colloidal gold staining (Bio-Rad, Hercules, CA). Quantitation was performed with an Image Station 1000 (Eastman Kodak, New Haven CT). Statistical analyses were performed using Excel (Microsoft, Redmond, WA) and SPSS (SPSS, Inc., Chicago, IL).

Immunohistochemistry

After rehydration, specimens were microwaved for 8 minutes at 300 W in 1 M sodium citrate, pH 6.4. Sections were probed with anti-p66^{Shc}, anti–proliferating cell nuclear antigen (PCNA; Zymed, South San Francisco, CA), anticleaved poly(adenyl ribose) polymerase (PARP; Cell Signaling Technologies, Beverly, MA), anti–pan-cytokeratin (Sigma), and/or anti–α-smooth muscle actin (Sigma) antibodies followed by Alexa 488–conjugated antirabbit and Alexa 594–conjugated antimouse IgG antibodies (Molecular Probes, Eugene, OR) (8). Autofluorescence was quenched in 10 mM $CuSO_4$, 50 mM CH_3COONH_4. To confirm specificity, sections were probed with anti-p66^{Shc} antibody preadsorbed to immunizing peptide at 1:20 wt/wt.

RESULTS

Normal Baboon Lung Development

To determine whether Shc isoforms are independently regulated in the fetal primate lung, specimens of normal baboon fetal lung were assessed by Shc Western analysis (Figure 1A and Figure E1 on the online supplement). Baboon lung homogenates contain

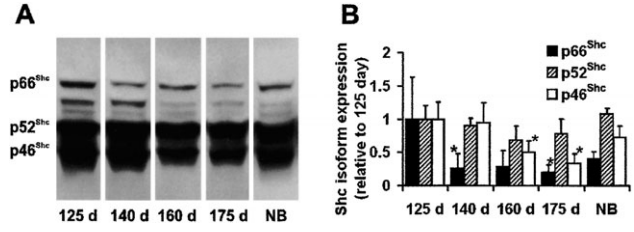

Figure 1. Shc isoform expression is developmentally regulated. Western analysis (*A*) and densitometry (*B*) were performed on normal baboon lungs at 125, 140, 160, and 175 days' gestation (term = 185 days), and postpartum (newborn, NB). p66^{Shc} content decreased with maturation ($p = 0.011$). Relative to Day 125, mean p66^{Shc} content decreased 74% by Day 140, 71% by Day 160, and 80% by Day 175 (*$p = 0.05$). *Error bars* represent SD throughout this report. Expression of p46^{Shc} fell 67% over the same period. p66^{Shc} expression increased 2.02-fold ($p = 0.034$) after Day 175. Changes in p52^{Shc} content were not statistically significant.

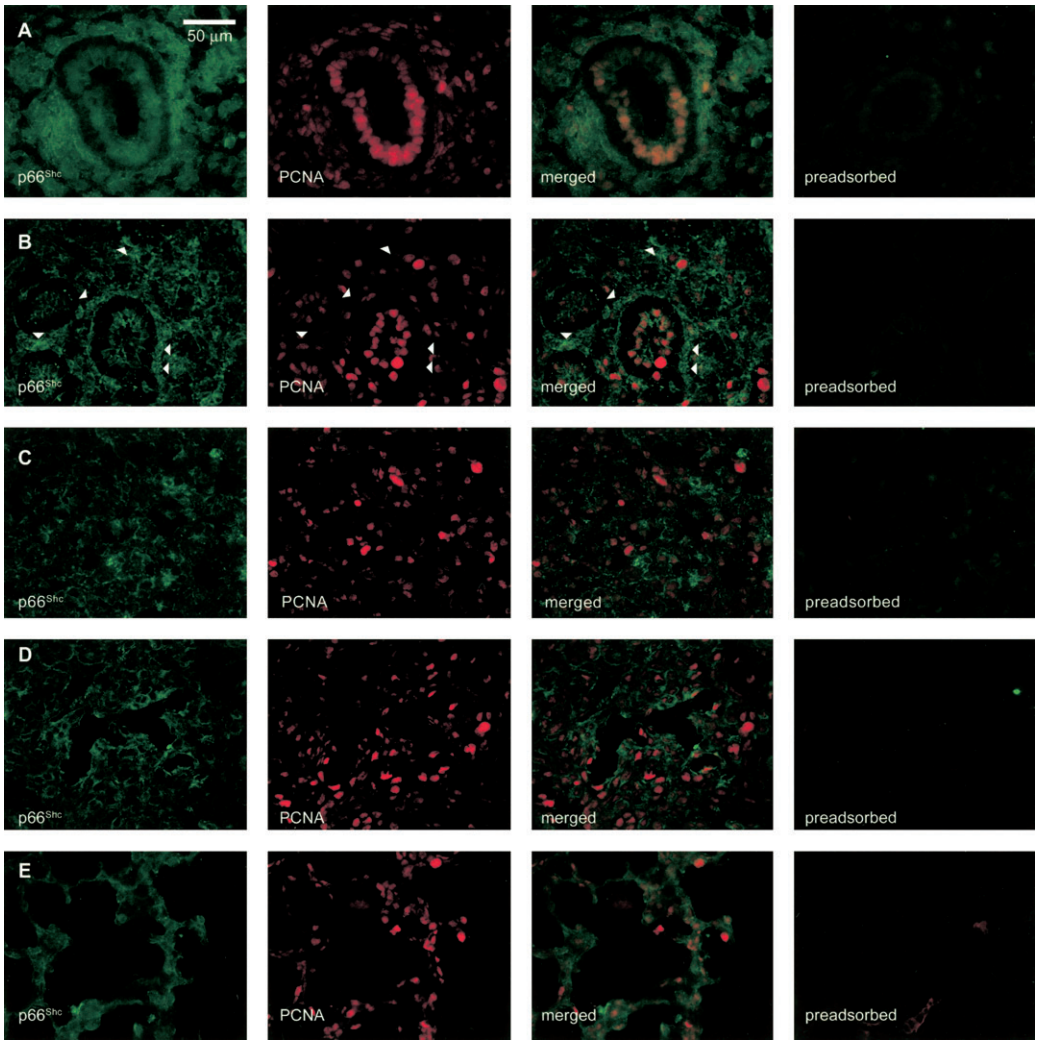

Figure 2. Epithelial p66^{Shc} and proliferating cell nuclear antigen (PCNA) expression both dissipate with maturation of the fetal baboon lung. By immunohistochemistry, p66^{Shc} (*green*) was ubiquitously expressed in the 60-day lung (*A*). PCNA (*red*) was sparse in mesenchymal cells but widespread among epithelial cells. By 90 days, p66^{Shc} was reduced and restricted to peribronchiolar mesenchymal cells and the apical cytoplasm of epithelial cells (*B*). PCNA expression persisted in most epithelial cells and increased in mesenchymal cells. Mesenchymal cells with high p66^{Shc} content (*arrowheads*) tended to express less PCNA. Between 125 (*C*) and 175 (*D*) days, p66^{Shc} expression shifted from isolated clusters of mesenchymal cells to discontinuous epithelial areas. Lungs from 140- and 160-day fetuses yielded variable and intermediate phenotypes in which p66^{Shc} is expressed in clusters of both epithelial and mesenchymal cells. During this period, cells expressing PCNA continued to be scattered throughout the lung. The 3-day postnatal lung (*E*) expressed little p66^{Shc}, and isolated cells expressing PCNA were scattered throughout the lung. Otherwise identically processed sections probed with preadsorbed p66^{Shc} antibody yielded minimal fluorescence.

proteins recognized by antibodies specific for the human and murine Shc SH2 domains, and whose migration corresponded to human and murine p66^{Shc}, p52^{Shc}, and p46^{Shc} isoforms. Two additional bands migrating between p52^{Shc} and p66^{Shc} were also detected, and may represent alternative Shc gene products unique to baboons. The p52^{Shc} and p46^{Shc} isoforms were more highly expressed than the p66^{Shc} isoform. The expression of p66^{Shc} decreased significantly between 125 and 160 days' gestation ($p =$

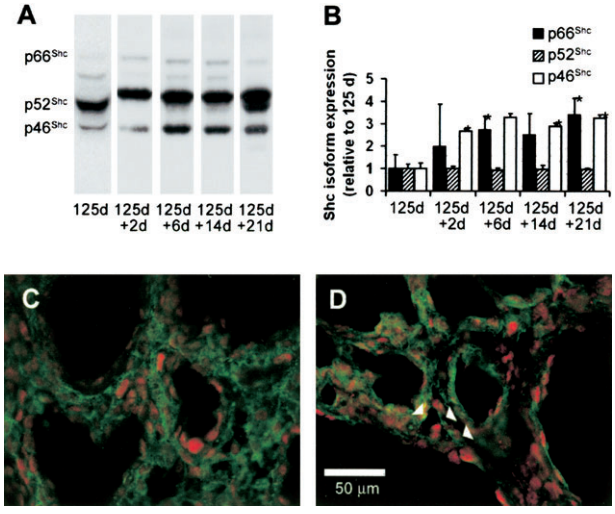

Figure 3. Shc isoform expression in a baboon model of mildly fibrotic bronchopulmonary dysplasia (BPD). Animals were delivered at 125 days' gestation and maintained up to 21 days with minimal trauma and supplemental oxygen. Shc Western analysis (*A*) and densitometry (*B*) indicate that, over this period, p66^{Shc} expression increased by 3.6-fold and p46^{Shc} by 3.3-fold (*$p < 0.05$). By immunohistochemistry, p66^{Shc} (*green*) primarily localized to the mesenchyme of normal 125-day gestation lungs (C), whereas PCNA (*red*) primarily localized to the epithelium. In contrast, p66^{Shc} was more strongly expressed in the epithelium of animals delivered at 125 days' gestation and maintained for 14 days *ex utero* (*D*). Staining is also intense in the endothelium of developing blood vessels (*arrowheads*). PCNA expression increased in mesenchymal cells and persisted in epithelial cells.

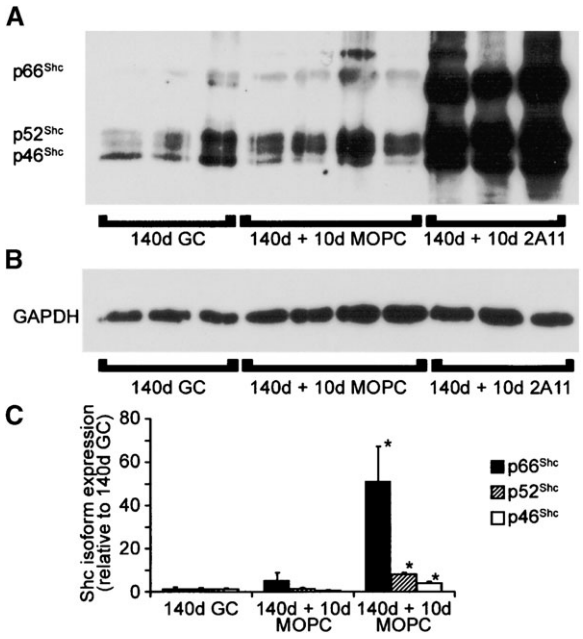

Figure 4. Shc isoform expression in the severely fibrotic baboon BPD model. Animals delivered at 140 days' gestation (gestational control, GC) and exposed to 100% oxygen for 10 days were infused with 5 mg/kg of either anti– bombesin-like peptide antibody (2A11) or nonimmune isotype-matched IgG (MOPC-21). 2A11 treatment clinically and pathologically attenuates BPD. Samples were equilibrated by total protein content, then analyzed by Shc Western analysis (*A*) and densitometry (*C*). Baboon lungs treated with MOPC-21 demonstrated 4.8-fold higher p66^{Shc} expression relative to gestational control lungs; this difference approached statistical significance ($p = 0.059$). In contrast, 2A11 treatment increased p52^{Shc} by sixfold, p46^{Shc} by sevenfold, and p66^{Shc} by tenfold (*$p < 0.003$ for all) relative to MOPC-21 control lungs, suggesting isoform-specific regulation ($p = 0.0073$). Glyceraldehyde phosphate dehydrogenase (GAPDH) reprobe of the Shc blot (*B*) confirmed equivalent total protein loading.

0.011 by one-way analysis of variance (ANOVA; Figure 1B) (16). Relative to Day 125, average p66^{Shc} protein content decreased 74% by Day 140, 71% by Day 160, and 80% by Day 175. Four specimens obtained 1 to 3 days after term delivery at 185 days were pooled for analysis (newborn, NB). Between 175 days' gestation and the immediate postpartum period, p66^{Shc} expression increased by a factor of 2.02 ($p = 0.034$ by *t* test, assuming equal variances) (17), suggesting upregulation of p66^{Shc} expression with term delivery. Similarly, average p46^{Shc} expression decreased 67% from 125 to 175 days' gestation ($p = 0.00008$ by ANOVA). Expression of p52^{Shc} decreased 31% between 125 and 160 days' gestation, but this change did not achieve statistical significance.

The localization of p66^{Shc} was evaluated in early fetal baboon lung using an isoform-specific antibody directed against the p66^{Shc} CH2 domain (8). Because p66^{Shc} putatively antagonizes cell proliferation, sections were also assessed for expression of PCNA, an indicator of cell replication (18). In the 60-day lung, p66^{Shc} was highly expressed in both epithelial and mesenchymal cells (Figure 2A). PCNA expression was widespread among epithelial cells and relatively sparse in the mesenchyme. By 90 days, overall p66^{Shc} expression had decreased considerably (Figure 2B). Although most cells expressed some p66^{Shc}, high-level expression was restricted to the mesenchyme directly adjacent to the incipient airways and moderate expression was present in the apical cytoplasm of epithelial cells. PCNA expression persisted in the epithelium and was moderately increased in the mesenchyme. The expression of p66^{Shc} continued to decrease through 125 days (Figure 2C), at which time p66^{Shc} expression was largely mesenchymal with little epithelial localization. Subsequently, mesenchymal expression diminished, whereas epithelial expression became more prominent through 140 and 160 days' gestation. By 175 days (Figure 2D), overall p66^{Shc} expression was restricted to isolated epithelial cells. PCNA expression concomitantly shifted from groups of epithelial cells to isolated epithelial and mesenchymal cells. Three days after term delivery at 185 days (Figure 2E), little p66^{Shc} was evident and PCNA expression remained scattered through the lung.

Because p66^{Shc} has also been described as mediating oxidative stress–induced cell death, its expression was also compared with that of cleaved PARP, a nuclear protein involved in DNA repair whose proteolysis is an early indicator of apoptosis (19). Although PARP cleavage is associated with p66^{Shc} signaling (20), minimal PARP proteolysis was identified at any stage of baboon lung development despite robust early p66^{Shc} expression (Figure E2).

These results suggest that Shc isoforms are independently regulated during baboon lung development, and that expression of p66^{Shc} and p46^{Shc} decrease with maturation. Localization of p66^{Shc} also shifts during lung development. In the baboon lung, the saccular stage begins at approximately 125 days and proceeds to 160 days. Pulmonary p66^{Shc} and p46^{Shc} expression are therefore downregulated in the baboon lung at a developmental stage similar to that of the mouse lung. In the mesenchyme, p66^{Shc} expression appeared to correlate inversely with PCNA expression, consistent with its putative function as a mitogenic inhibitor. However, epithelial PCNA expression persisted despite high p66^{Shc} levels.

Mildly Fibrotic 125-Day Baboon BPD Model

Having demonstrated that Shc isoform expression is modulated during normal lung development, we hypothesized that this regulation may be altered by premature birth and the subsequent onset of neonatal chronic lung disease. To evaluate this postulate, specimens were obtained from baboons delivered prematurely at 125 days' gestation and maintained for up to 21 days under a protocol developed to replicate the mildly fibrotic BPD associated with extremely premature delivery and current clinical practice (14). In this model, oxygen was administered only as clinically indicated to maintain transcutaneous oxygen saturations at approximately 90%, and barotrauma was minimized. Shc expression was assessed by Western analysis (Figures 3A and 3B). Unlike the decrease in p66^{Shc} and p46^{Shc} content observed during normal lung development, p66^{Shc} and p46^{Shc} expression increased in the 21 days after premature delivery. The expression of p66^{Shc} and p46^{Shc} increased by factors of 3.6 ($p = 0.025$ by one-way ANOVA) and 3.3 ($p = 0.0000024$ by one-way ANOVA), respectively. In contrast, the expression of p52^{Shc} over the same period was remarkably consistent, varying by less than 7%. Isoform-specific immunohistochemistry also demonstrated a change in p66^{Shc} localization. In normal 125-day fetal baboons, p66^{Shc} was distributed throughout the lung, with higher expression in mesenchymal cells (Figure 3C), whereas PCNA was primarily expressed in the epithelium. In contrast, animals maintained for 14 days *ex utero* expressed p66^{Shc} most strongly in the epithelium (Figure 3D). PCNA was evident throughout the lungs of these animals. Cleaved PARP expression was also evaluated but not detected (Figure E3). Because epithelial and mesenchymal cells may become interspersed with BPD, p66^{Shc} localization was confirmed by colocalization with cytokeratin and with α–smooth muscle actin (Figure E3). Interestingly, p66^{Shc} tended not to colocalize with α–smooth muscle actin, even when strongly expressed in adjacent mesenchymal cells. Mesenchymal p66^{Shc} labeling was most intense in the endothelium of

developing vessels. Modest parenchymal thickening was evident, but fibrotic changes were minimal. Intracellular distribution was cytoplasmic, consistent with previous descriptions of Shc intracellular localization (21).

Severely Fibrotic 140-Day Baboon BPD Model

Shc expression was also evaluated in a model of severely fibrotic BPD in which baboons are delivered prematurely at 140 days' gestation and maintained on 100% oxygen for 10 days (140 days/100% oxygen). Animals subjected to this protocol develop severe BPD similar to that originally described by Northway and colleagues (9). In this model, the clinical and pathologic severity of lung injury is attenuated by intravenous infusions of 2A11, an anti-BLP antibody (11). To determine whether Shc isoform expression is altered by 2A11 treatment in parallel with BPD abrogation, Shc content was assessed by Western analysis (Figure 4A). Samples were equalized by total protein content, and equivalent loading subsequently confirmed by glyceraldehyde phosphate dehydrogenase Western analysis (Figure 4B). Relative to 140-day gestational control animals, $p66^{Shc}$ expression was 4.8-fold higher in 10-day-old 140-day/100% oxygen severely fibrotic BPD baboons treated with MOPC-21 nonimmune control antibody (Figure 4C). This difference approached statistical significance ($p = 0.059$ by t test after log transformation). In contrast, otherwise identically treated animals receiving 2A11 had dramatically increased absolute and relative $p66^{Shc}$ expression. Although animals receiving 2A11 respectively yielded 6.2- and 7.1-fold higher $p52^{Shc}$ and $p46^{Shc}$ expression relative to 140-day/100% oxygen MOPC-21 baboons ($p < 0.002$ by t test for both), $p66^{Shc}$ expression increased 10.5-fold ($p = 0.0026$ by t test). Regulation of $p66^{Shc}$ differed significantly from that of the other isoforms ($p = 0.0073$ by two-way ANOVA) (16). These findings suggest that 2A11 attenuates clinical and pathologic signs of BPD while disproportionately increasing $p66^{Shc}$ expression.

Tissue localization of $p66^{Shc}$, PCNA, and cleaved PARP were also evaluated in this model. In the normal 140-day fetal baboon lung (Figure 5A), $p66^{Shc}$ and PCNA were expressed in both epithelial and mesenchymal cells. Cleaved PARP expression was sparse and localized to isolated epithelial cells, coincident with high $p66^{Shc}$ expression (Figure 6A). Animals exposed to supplemental oxygen for 10 days only as clinically indicated developed minimal fibrosis and yielded patterns of $p66^{Shc}$, PCNA, and cleaved

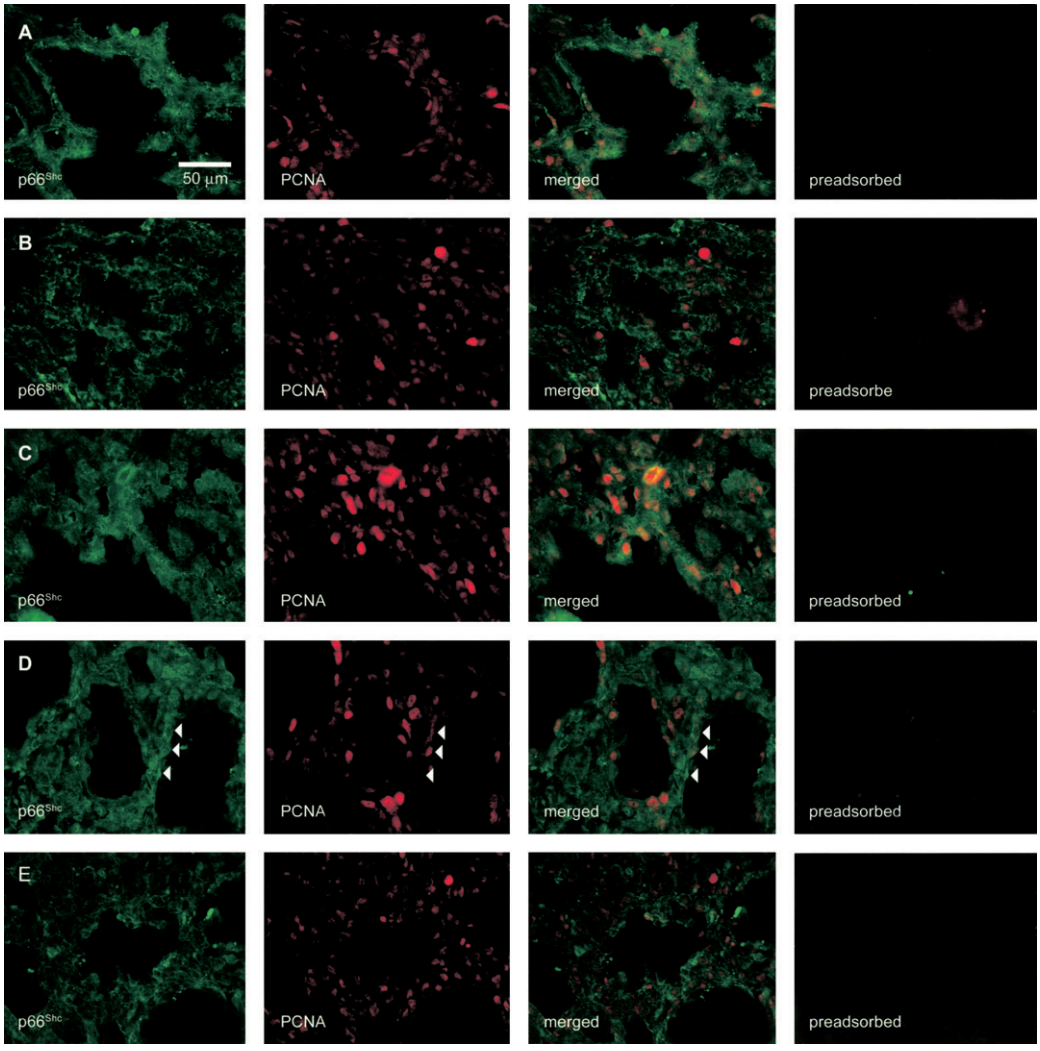

Figure 5. Localization of $p66^{Shc}$ shifts from the epithelium to the mesenchyme with induction of severely fibrotic BPD. Baboons were delivered at 140 days' gestation, exposed to 100% oxygen for 10 days, and treated with 2A11 or MOPC-21 control antibody as described previously. Minimal fibrosis was evident in 140-day animals exposed to supplemental oxygen only as clinically indicated for 10 days, or in normal 140- and 160-day fetal lungs. Lung specimens were evaluated for $p66^{Shc}$ and PCNA immunolocalization. In 140-day gestation lungs, $p66^{Shc}$ (*green*) was strongly expressed in isolated epithelial cells, with lower expression throughout the rest of the lung (*A*). PCNA (*red*) was present in most cells but more prominent in the epithelium. Similar patterns of $p66^{Shc}$ and PCNA localization were evident in baboons subjected to oxygen only as clinically indicated (*B*). In contrast, $p66^{Shc}$ localized to mesenchymal cells in 10-day-old animals treated with 100% oxygen and MOPC-21 (*C*). PCNA expression increased and was most prominent in the mesenchyme. Baboons receiving 100% oxygen and anti-bombesin antibody (2A11) continued to express $p66^{Shc}$ primarily in epithelial cells (*D*). PCNA expression was lower than in animals receiving MOPC-21 and most evident in the epithelium. Although both $p66^{Shc}$ and PCNA localized to the epithelium, epithelial cells with high $p66^{Shc}$ content (*arrowheads*) tended to express PCNA. Both $p66^{Shc}$ and PCNA were expressed throughout the lung at low levels in the 160-day baboon (*E*). Otherwise identically processed sections probed with preadsorbed $p66^{Shc}$ antibody and without PCNA antibody yielded minimal fluorescence.

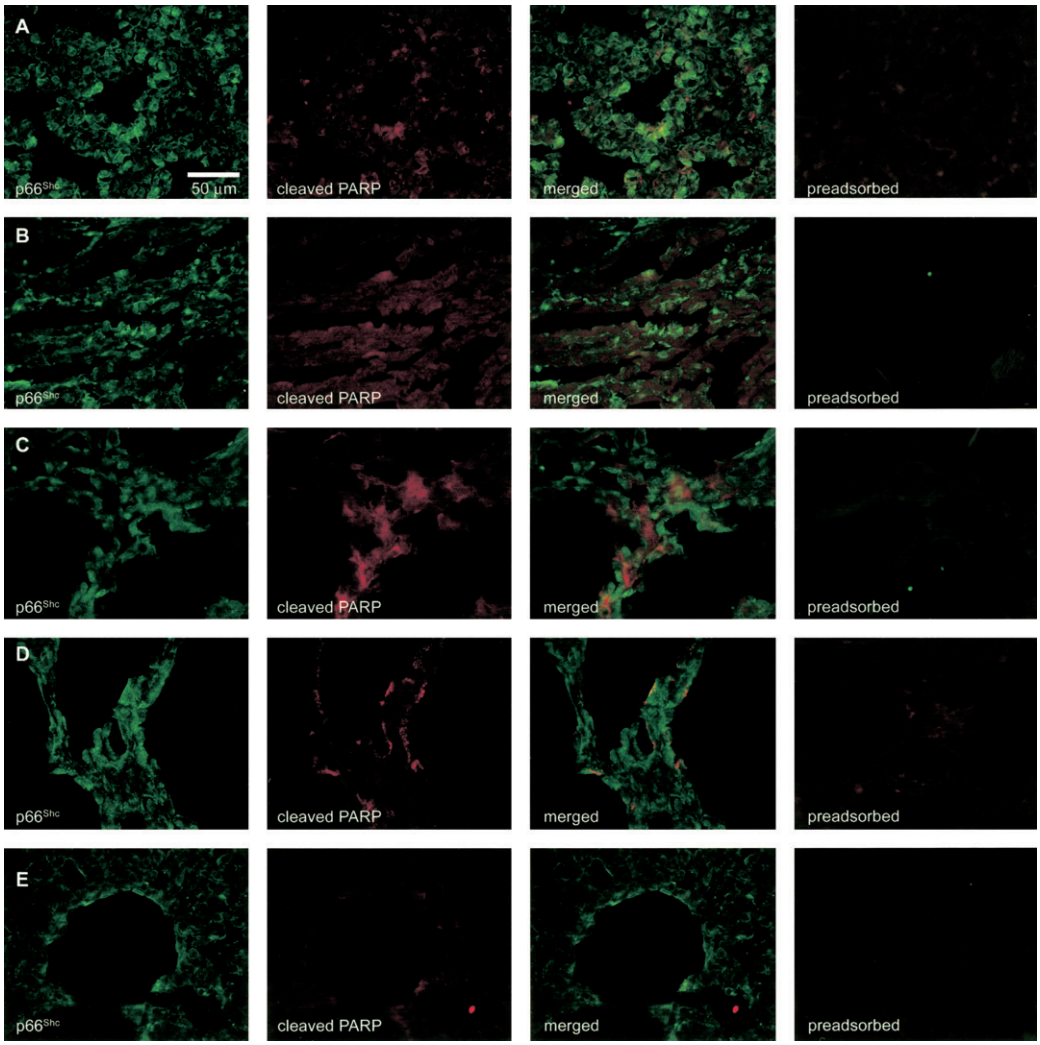

Figure 6. Poly(adenyl ribose) polymerase (PARP) is cleaved within tissues expressing p66^{Shc} in the severely fibrotic BPD model. PARP proteolysis is an early indicator of apoptosis. Baboons were delivered at 140 days' gestation, exposed to 100% oxygen for 10 days, and treated with 2A11 or MOPC-21 antibodies as described previously. Lung sections were evaluated for p66^{Shc} and PCNA immunolocalization. In the 140-day–gestation lung (*A*), both p66^{Shc} (*green*) and cleaved PARP (*red*) were most prominent in isolated epithelial cells. However, individual cells rarely expressed both epitopes. Premature birth and exposure to 10 days of minimal oxygen as clinically indicated resulted in minimally fibrotic BPD and undetectable PARP proteolysis (*B*). In contrast, induction of fibrotic BPD by exposure to 100% oxygen for 10 days (and infusion of MOPC-21 nonimmune antibody) increased PARP proteolysis (*C*). Cleaved PARP and p66^{Shc} both localized to the mesenchyme, but generally to different cells. Attenuation of BPD by administering the anti-bombesin antibody 2A11 to animals exposed to 100% oxygen (*D*) shifted both PARP proteolysis and p66^{Shc} expression to the epithelium. In these lungs, cleaved PARP was sparse and immunolocalized to the apical cytoplasm of cells expressing p66^{Shc}. Finally, normal 160-day–gestation baboon lung (*E*) did not demonstrate PARP proteolysis. For each condition, otherwise identically processed sections probed with preadsorbed p66^{Shc} antibody and without anticleaved PARP antibody yielded minimal fluorescence.

PARP localization similar to those of 140-day gestational control animals (Figures 5B and 6B). In contrast, 140-day animals exposed to 100% oxygen and infused with either no antibody (not shown) or with MOPC-21 expressed p66^{Shc}, PCNA (Figure 5C), and cleaved PARP (Figure 6C) in clusters of mesenchymal cells within fibrotic interalveolar septa. Cleaved PARP tended to localize to mesenchymal cells with low p66^{Shc} content. Cells expressing p66^{Shc} were not derived from vascular endothelium, as inferred by a lack of coexpressed platelet endothelial cell adhesion molecule-1 (data not shown). This shift in p66^{Shc} localization did not occur in otherwise identical animals treated with 100% oxygen and 2A11 anti-BLP antibody. In these animals, p66^{Shc}, PCNA (Figure 5D), and cleaved PARP (Figure 6D) continued to be expressed in the epithelium. Moreover, PCNA expression and PARP proteolysis were both diminished by 2A11 treatment. In the normal 160-day baboon lung, p66^{Shc} was also localized to epithelial cells (Figure 5E); cells with strong PCNA expression were rare, and PARP proteolysis was undetectable. Tissue localization of p66^{Shc} was further confirmed by coimmunolocalization with cytokeratin and with α–smooth muscle actin (Figures E4 and E5, respectively). Again, p66^{Shc} tended not to colocalize with α–smooth muscle actin, even when strongly expressed in the mesenchyme. These findings suggest that p66^{Shc}, PCNA, and cleaved PARP localization shift from the epithelium to the mesenchyme with induction of classical BPD, and that this shift is prevented by adsorption of circulating BLPs.

Normal Human Lung Development

To determine whether isoform-specific Shc regulation is also relevant to human lung development, snap-frozen samples were obtained from the lungs of 12 normal human fetuses whose gestational ages ranged from 18 to 24 weeks. Isoform-specific Shc regulation was assessed by Western analysis (Figure 7A). Samples were equalized by total protein content and equivalent loading confirmed by colloidal gold staining and glyceraldehyde phosphate dehydrogenase reprobe (Figure E6). The expression of p52^{Shc} and p46^{Shc} was higher than that of p66^{Shc}, necessitating longer chemiluminescence exposure times to evaluate p66^{Shc} expression. The highest levels of p66^{Shc} expression were observed before 21 weeks' gestation, after which p66^{Shc} content fell dramatically (Figure 7B; $p = 0.02$ by one-way ANOVA). Average p66^{Shc} expression was maximal and nearly identical at 18 and 20 weeks. Subsequently, expression decreased 12% by 21 weeks, 42% by 22 weeks, and 87% by 24 weeks. In contrast, p52^{Shc} and p46^{Shc} expression were relatively consistent across all gestational ages, with all values within 27% of the mean.

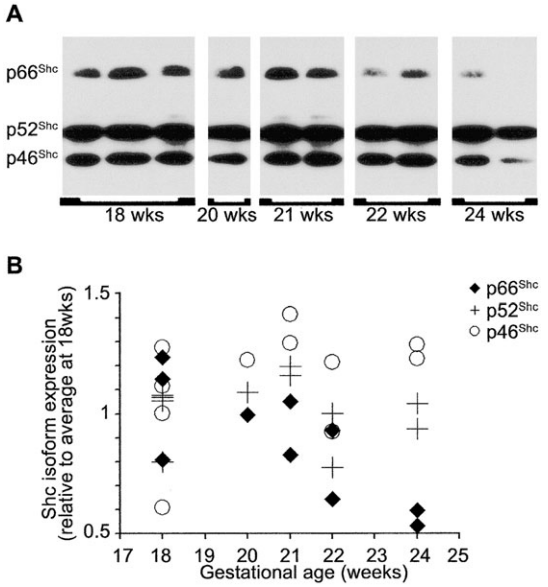

Figure 7. Expression of p66^{Shc} is developmentally regulated in the human lung. Shc Western analysis (*A*) and densitometry (*B*) were performed on snap-frozen lung samples obtained from normal human fetuses at 18 to 24 weeks' gestation. Expression of p52^{Shc} and p46^{Shc} were greater than that of p66^{Shc}, necessitating different exposures of the same blot. p66^{Shc} content decreased significantly over this period ($p = 0.02$). Average p66^{Shc} expression was maximal at 18 and 20 weeks, decreasing 12% by 21 weeks, 42% by 22 weeks, and 87% by 24 weeks. In contrast, p52^{Shc} and p46^{Shc} were relatively consistent, with all values within 27% of the mean.

Normal human fetal lung specimens were also evaluated by p66^{Shc} immunostaining, which demonstrated widespread expression of p66^{Shc} throughout the 18-week lung (Figure 8A). p66^{Shc} was particularly prominent within epithelial cells lining the primitive airspaces. PCNA and p66^{Shc} were widely coexpressed in the epithelium, similar to the normal 125-day baboon lung (Figure 2C). At 20 weeks (Figure 8B), the contrast between the epithelium and the mesenchyme became progressively more distinct, reflecting diminished mesenchymal expression. Moreover, within highly expressing cells, p66^{Shc} labeling was less homogeneous and assumed a more apical distribution. PCNA was again expressed in most epithelial cells and in isolated mesenchymal cells.

Subsequently, the proportion of epithelial cells expressing high levels of p66^{Shc} immunostaining decreased with maturation. Although most cells in the 22-week lung exhibited low concentrations of p66^{Shc}, high-level expression was restricted to occasional cells in both the epithelial and mesenchymal compartments (Figure 8C). Epithelial PCNA expression diminished in parallel with p66^{Shc} expression but continued to be expressed in isolated mesenchymal cells. By 24 weeks, much of the mesenchyme had involuted (Figure 8D). Relatively few epithelial cells continued to express high levels of p66^{Shc}, and some mesenchymal cell populations expressed no detectable p66^{Shc}, as is evident from the dark regions scattered throughout the parenchyma. PCNA became further restricted to isolated epithelial and mesenchymal cells.

The progressive restriction of p66^{Shc} expression to epithelial cells during human lung development recapitulates p66^{Shc} immunolocalization in 125- and 140-day baboon lungs, and the quantitative decrease in p66^{Shc} expression demonstrated by Western analysis correlates with decreasing epithelial p66^{Shc} localization. PCNA expression in developing human pulmonary epithelium decreased in parallel with p66^{Shc} expression, also recapitulating the pattern observed in the developing baboon lung. However, the maturational increase in mesenchymal PCNA expression observed in the baboon lung was not apparent in humans.

Tissue localization of p66^{Shc} was confirmed by coimmunolocalization of cytokeratin (Figure E7) and α–smooth muscle actin (Figure E8). Again, mesenchymal cells expressing p66^{Shc} did not simultaneously express α–smooth muscle actin.

p66^{Shc} was also coimmunolocalized with cleaved PARP in these samples. PARP proteolysis was sparse at all gestational ages (Figure E9). When present, cleaved PARP tended to be expressed in mesenchymal cells with low p66^{Shc} content.

Human Postmortem BPD Lungs

To evaluate p66^{Shc} expression in the prematurely delivered human lung, autopsy specimens were evaluated by p66^{Shc}, PCNA, and cleaved PARP immunolocalization. Autopsies were performed within 6 hours of death, and clinical synopses are listed in Table 1. Postmortem lung specimens were selected from four cases whose final pathologic diagnoses included bronchopulmonary dysplasia, including one (Case 4) with a clinical history and postmortem findings characteristic of severe fibrotic BPD. For comparison, specimens were also obtained from term and premature infants succumbing to sepsis or other nonpulmonary causes, and whose histologic diagnoses did not include BPD or chronic lung disease. Most infants diagnosed with BPD were considerably older than the non-BPD cases at the time of death. Specimens from all three categories demonstrated p66^{Shc} expression in most cells, with varying populations of highly expressing cells. The distribution and the proportions of highly expressing cells were consistent within regions of similar tissue morphology.

In near-term newborn infants without lung disease (Figures 9A and 10A; Case 2, a 4-day-old ex–36-week infant), interalveolar septa were thin, with little mesenchyme. Although nearly all cells expressed some p66^{Shc}, a population of intensely labeled cells were scattered throughout the mesenchyme. Within these cells, p66^{Shc} localized to a nuclear or perinuclear distribution. This localization contrasts with that of the prenatal lung, in which epithelial expression is more prominent. PCNA expression was limited to scattered cells (predominantly epithelial), and PARP cleavage was undetected.

Newborn preterm infants had thicker septa with more mesenchyme (Figures 9B and 10B; Case 9, a 1-day-old ex–27-week infant) than term newborns. Moderate levels of p66^{Shc} were present in most mesenchymal cells, and high-level expression was apparent in scattered epithelial cells. PCNA expression was limited to isolated epithelial cells, and PARP proteolysis was not observed. Older premature infants without clinical or pathologic BPD (Figures 9C and 10C; Case 10, a 32-day-old ex–28-week infant) had thinner interalveolar septa, but continued to exhibit moderate p66^{Shc} labeling of most mesenchymal cells and increased expression within scattered epithelial cells. Cells expressing PCNA were sparse and mostly epithelial; again, PARP cleavage was undetectable.

In contrast, the lungs of a 13-day-old ex–28-week premature infant with early evolving BPD (Figures 9D and 10D, Case 7) had thickened septa with heterogeneously labeled mesenchymal cells. Most prominent, however, were continuous lines of strongly expressing epithelial cells. This expression pattern was reminiscent of the 18- to 22-week human fetal lung. Overall, the prevalence of highly expressing cells was greater than in lungs without BPD. However, PCNA expression and PARP cleavage remained low.

In an older patient with mildly fibrotic BPD (Figures 9E and 10E; Case 5, a 60-day-old ex–26-week infant), p66^{Shc} localized

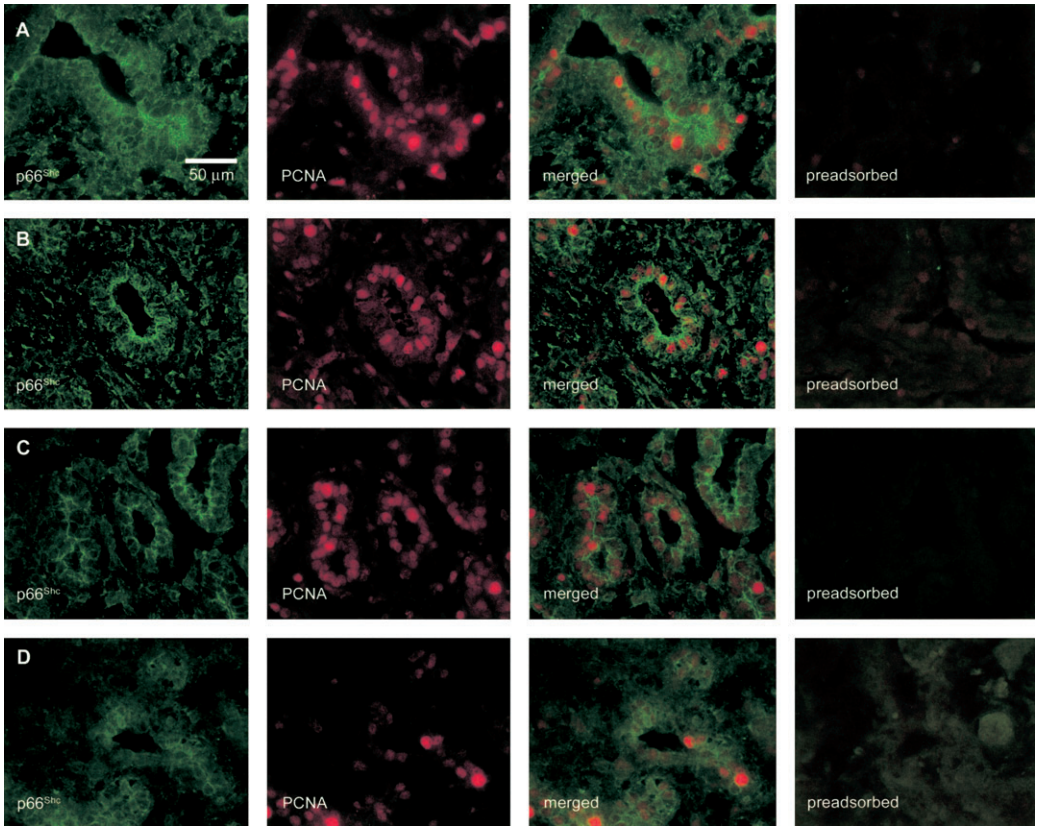

Figure 8. Immunolocalization of p66^{Shc} and PCNA change during normal human lung development, recapitulating observations in the fetal baboon. Expression of p66^{Shc} in the 18-week lung (*A*) was maximal, widespread, and prominent within the epithelium of primitive airspaces. In the 20-week lung (*B*), p66^{Shc} expression was decreased and localized to scattered mesenchymal cells and the apical cytoplasm of most epithelial cells. At 22 weeks (*C*), some areas of the mesenchyme expressed minimal p66^{Shc}, and high-level expression remained restricted to the apical cytoplasm of scattered epithelial cells. In the 18-, 20-, and 22-week lungs, PCNA was expressed throughout the epithelium, with only isolated mesenchymal expression. By 24 weeks (*D*), high-level p66^{Shc} expression was further restricted to isolated clusters of epithelial cells, and mesenchymal expression was sparse and patchy. PCNA expression also became sparse and was now scattered through the lung. Otherwise identically processed sections probed with preadsorbed p66^{Shc} antibody and without anti-PCNA antibody yielded minimal fluorescence.

to continuous lines of strongly expressing epithelial cells. As in early BPD, the mesenchymal compartment was heterogeneously labeled, with patches of strongly expressing cells adjoining areas of minimal expression. Highly labeled macrophages were also evident. PCNA expression and PARP proteolysis were both increased, and most prominent among epithelial cells. In contrast, the patient with histologic findings and a clinical course consistent with classical severe fibrotic BPD (Figures 9F and 10F; Case 4, a 97-day-old ex–27-week infant) expressed p66^{Shc} primarily in the mesenchyme, with relatively little epithelial or endothelial expression. Although areas of highly expressing cells were scattered throughout the mesenchyme, most mesenchymal cells expressed moderate levels of p66^{Shc}. PCNA expression was very low, and PARP cleavage was undetectable.

p66^{Shc} tissue localization was again confirmed by coimmunolocalization with cytokeratin (Figure E10) and α–smooth muscle actin (Figure E11). As in the baboon BPD model, mesenchymal cells expressing p66^{Shc} did not simultaneously express α–smooth muscle actin.

In both fibrotic and nonfibrotic BPD, intracellular p66^{Shc} localization was cytoplasmic, and not perinuclear as in normal lungs or lungs with acute disease. The distribution of p66^{Shc} in the patient with severe BPD was similar to that of baboons delivered at 140 days and treated with 100% oxygen for 10 days. Expression of p66^{Shc} in the patients with mildly fibrotic BPD resembled that of baboons delivered at 125 days' gestation and maintained with oxygen only as needed. These findings indicate that, in both humans and baboons, p66^{Shc} expression and localization change with premature birth and the pathogenesis of chronic lung disease.

DISCUSSION

Our findings support the hypothesis that pulmonary p66^{Shc} expression is developmentally regulated in baboons and humans as well as in mice. For all three species, p66^{Shc} expression is highest in the early fetal lung and decreases with maturation. In the mouse lung, p66^{Shc} expression decreases just before birth at 18.5 days' gestation, during the early saccular stage of development (22). By comparison, p66^{Shc} decreased through the saccular stage of baboon lung development (14) and during the late canalicular stage of human lung development (23). At the end of gestation, mice have saccular stage lungs, whereas term baboon and human infants have begun alveolarization. Thus, differences in the timing of p66^{Shc} downregulation reflect differences in the ontogeny of lung development within each species. Conservation of the three Shc isoforms and their developmental regulation across taxonomic orders suggests that p66^{Shc} regulates lung development in many mammalian species, and that attenuation of p66^{Shc} before birth is adaptive.

After premature delivery, p66^{Shc} expression in the premature lung correlated inversely to the degree of fibrosis. Relatively little p66^{Shc} was expressed in 140-day–gestation baboons, and expression was mildly increased with induction of severely fibrotic BPD. Conversely, experimental attenuation of severe BPD using intravenous anti-BLP antibodies dramatically increased relative and absolute p66^{Shc} expression. Moreover, in the 125-day mildly fibrotic baboon BPD model, p66^{Shc} is high at birth and remains elevated for at least 21 days, rather than declining as it would *in utero*. Thus, in premature lungs, elevated p66^{Shc} expression was associated with a mildly fibrotic BPD

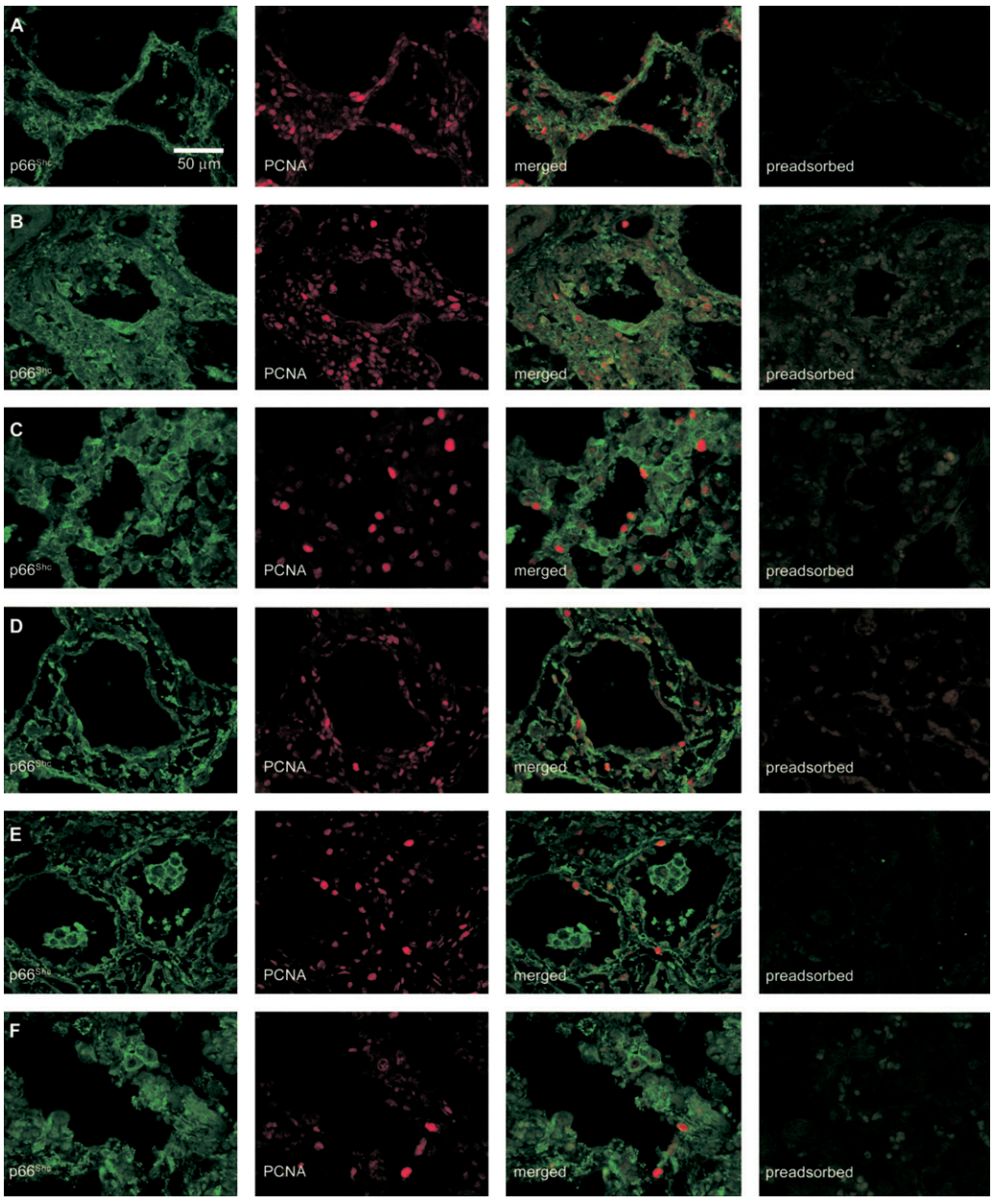

Figure 9. Immunolocalization of p66^{Shc} differs with human neonatal lung pathology and is reciprocal to that of PCNA. After term delivery without lung disease (*A*; Case 2, a 4-day-old ex–36-week infant), p66^{Shc} (*green*) localized to intensely labeled mesenchymal cells scattered amid more moderately labeled mesenchymal and epithelial populations, whereas occasional PCNA-positive cells predominantly localized to the epithelium. Within highly expressing cells, p66^{Shc} localizes in a nuclear or perinuclear distribution. After preterm delivery (*B*; Case 9, a 1-day-old ex–27-week infant), p66^{Shc} was diffusely expressed in the thickened mesenchyme and more prominent within epithelial cells. In contrast, PCNA localized to scattered mesenchymal cells. Healthy lungs of older premature infants (*C*; Case 10, a 32-day-old ex–28-week infant) were more similar to those of term newborns, with scattered epithelial cell expression and moderately labeled, thinner mesenchyme. Again, occasional PCNA-positive cells were scattered throughout the epithelium. A premature infant with early BPD (*D*; Case 7, a 13-day-old ex–28-week infant) exhibited continuous areas of epithelial p66^{Shc} expression and heterogeneous mesenchymal labeling within grossly thickened alveolar septa. PCNA was rare and limited to scattered epithelial and mesenchymal cells with lower p66^{Shc} expression. Progression to mildly fibrotic BPD (*E*; Case 5, a 60-day-old ex–26-week infant) was also associated with continuous strips of epithelial labeling and heterogeneous mesenchymal expression, as well as strongly positive alveolar macrophages. PCNA localized to scattered epithelial cells with low p66^{Shc} expression. In contrast, p66^{Shc} primarily localized to the mesenchyme of an older patient with severely fibrotic BPD (*F*; Case 4, a 97-day-old ex–27-week infant). Little epithelial p66^{Shc} labeling was evident. Cells expressing PCNA were also rare and generally located in the epithelium. In diseased lungs, intracellular p66^{Shc} localization was predominantly cytoplasmic, in contrast to the perinuclear distribution observed in normal lungs.

phenotype. We note that p66^{Shc} consistently failed to colocalize with α–smooth muscle actin, leading us to speculate that p66^{Shc} expression is inversely correlated to the differentiation of myofibroblast populations implicated in the pathogenesis of BPD (24).

In both humans and baboons, mild or minimally fibrotic lung disease was associated with epithelial p66^{Shc} localization. This change in p66^{Shc} localization parallels the shift in expression seen during normal lung development In contrast, baboons and the human with severely fibrotic BPD expressed p66^{Shc} primarily in the mesenchyme. Moreover, experimental attenuation of BPD in the 140-day/100% oxygen baboon BPD model using 2A11 anti-BLP antibody was associated with an epithelial p66^{Shc} distribution as well as greatly increased p66^{Shc} expression. Thus, loss of epithelial p66^{Shc} expression appears to correlate with mesenchymal expansion and the development of severely fibrotic BPD in both premature baboons and humans. The persistence of mesenchymal p66^{Shc} expression in the mildly fibrotic BPD model may reflect the degree to which normal lung development is disrupted.

The function of p66^{Shc} in the developing lung is likely to be related to its previously defined signaling functions. On tyrosine phosphorylation, p66^{Shc} binds and sequesters Grb2 (25), thereby antagonizing Ras activation by receptor tyrosine kinases. We

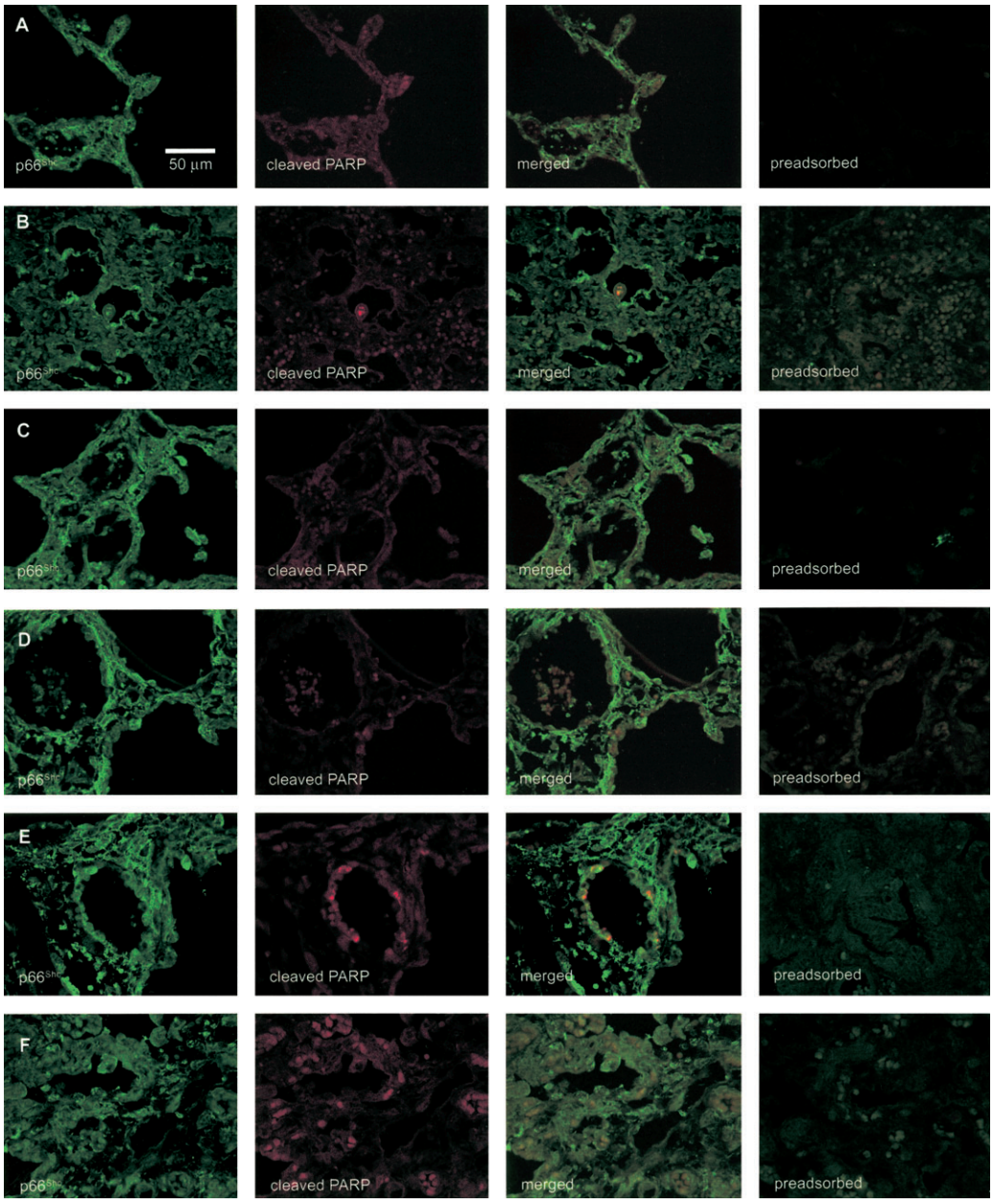

Figure 10. Cleaved PARP and p66^{Shc} are each upregulated but localize to opposing cells in evolving BPD. Pathologic sections described in Figure 9 were evaluated by p66^{Shc} and cleaved PARP immunohistochemistry. Minimal PARP proteolysis was observed in the healthy lungs of a full-term infant (*A*; Case 2, a 4-day-old ex–36-week infant), the undiseased lungs of a newborn premature infant (*B*; Case 9, a 1-day-old ex–27-week infant), the healthy lungs of older premature infants (*C*; Case 10, 32-day-old ex–28-week infant), or the lungs of a premature infant with early BPD (*D*; Case 7, a 13-day-old ex–28-week infant). Progression to mildly fibrotic BPD (*E*; Case 5, a 60-day-old ex–26-week infant) was associated with epithelial cleaved PARP labeling in contrast to the mesenchymal p66^{Shc} expression noted in Figure 9. Subsequently, minimal specific cleaved PARP immunoreactivity was detected in the lungs of an older infant with severe fibrotic BPD (*F*; Case 4, a 97-day-old ex–27-week infant). For each condition, otherwise identically processed sections probed with preadsorbed p66^{Shc} antibody and without anti-PARP antibody yielded minimal fluorescence.

speculate that expression of p66^{Shc} may represent inhibitory feedback on mitogenic signaling through MAP kinases. Thus, p66^{Shc} localization may indicate the proliferation of specific cell populations. A previous evaluation of lung cell proliferation in the mildly fibrotic 125-day baboon BPD model (26) supports this postulate. First, cell proliferation in the baboon decreases with maturation, falling 97% between Days 125 and 175. This drop parallels the decrease in p66^{Shc} expression over the same period. Second, cell proliferation in the mildly fibrotic 125-day baboon BPD model remains elevated through at least 21 days after birth, again closely paralleling the expression of p66^{Shc} in the same model. Finally, in the baboon BPD model, proliferating cells localize primarily to the epithelium through the first 14 days of life, coincident with p66^{Shc} immunolocalization. In the current study, p66^{Shc} consistently localized to the same tissues as PCNA, though often in different individual cells. We therefore speculate that p66^{Shc} expression represents the inhibitory limb of a feedback loop regulating cell proliferation in the BPD lung. Its expression in the mesenchyme of fibrotic lungs may therefore relate to ongoing proliferation within this compartment. Conversely, epithelial p66^{Shc} expression after 2A11 infusion appears to be independent of any initial increase in proliferation. In this population, Shc isoform expression may represent a mechanism by which bombesin signaling regulates epithelial cell mitogenesis.

p66^{Shc} also mediates oxidative stress signaling on serine phosphorylation, resulting in activation of the mitochondrial apoptosis pathway, culminating in caspase activation and cytochrome-*c* release (27, 28). In the current study, both cleaved PARP and p66^{Shc} localized to the mesenchyme of 140-day baboons with BPD, and attenuation of BPD in the same model shifted both p66^{Shc} and cleaved PARP expression to the epithelium. These findings are therefore broadly consistent with the putative role of p66^{Shc} in mediating oxidative stress responses. However, the large increase in p66^{Shc} expression associated with 2A11 treatment infers that its function in BPD is adaptive. In contrast, p66^{Shc} has been characterized as playing a maladaptive role in oxidative lung

disease. Mice deficient in $p66^{Shc}$ are resistant to oxidative injury from hydrogen peroxide and paraquat, and live 30% longer (7). Susceptibility to oxidative stress is restored by induced $p66^{Shc}$ expression. It is unclear how these findings may be reconciled; it is possible that p66Shc confers different functions in neonates and adults.

The expression and localization of $p66^{Shc}$ within the neonatal lung may therefore identify a population of cells that is both rapidly proliferating and at increased risk of oxidative stress–induced cell death. The shift of $p66^{Shc}$ expression from the epithelium to the mesenchyme in severely fibrotic BPD may directly regulate both cell populations. We note that many of the signaling pathways converging on Shc have been implicated in the regulation of lung cell proliferation and survival, including those of epidermal growth factor (29), insulin (4), and fibroblast growth factors (30). The elucidation of the mechanisms governing Shc isoform expression may provide additional insight into the determinants of pulmonary fibrosis after premature birth. Moreover, the signaling pathways converging on Shc may be manipulated to determine how mitogenic and oxidative stress signaling interact to regulate fibrogenic precursors.

***Conflict of Interest Statement*:** M.K.L. does not have a financial relationship with a commercial entity that has an interest in the subject of this manuscript; G.S.P. does not have a financial relationship with a commercial entity that has an interest in the subject of this manuscript; M.A.S. does not have a financial relationship with a commercial entity that has an interest in the subject of this manuscript; S.M.S. does not have a financial relationship with a commercial entity that has an interest in the subject of this manuscript; Z.P. does not have a financial relationship with a commercial entity that has an interest in the subject of this manuscript; M.E.S. does not have a financial relationship with a commercial entity that has an interest in the subject of this manuscript.

***Acknowledgment*:** Key R-10 support personnel include Vicki Winters and the pathology staff at University of Texas Health Sciences Center at San Antonio, and the Neonatal Intensive Care Unit and animal production staffs at the Southwest Foundation for Biomedical Research. Histology technical support was provided by Pablo Bringas Jr. and Valentino Santos of the University of Southern California Center for Craniofacial Molecular Biology.

References

1. Pelicci G, Lanfrancone L, Grignani F, McGlade J, Cavallo F, Forni G, Nicoletti I, Pawson T, Pelicci PG. A novel transforming protein (SHC) with an SH2 domain is implicated in mitogenic signal transduction. *Cell* 1992;70:93–104.
2. Migliaccio E, Mele S, Salcini AE, Pelicci G, Lai KM, Superti Furga G, Pawson T, di Fiore PP, Lanfrancone L, Pelicci PG. Opposite effects of the p52shc/p46shc and p66shc splicing isoforms on the EGF receptor-MAP kinase-fos signalling pathway. *EMBO J* 1997;16:706–716.
3. Batzer AG, Rotin D, Urena JM, Skolnik EY, Schlessinger J. Hierarchy of binding sites for Grb2 and Shc on the epidermal growth factor receptor. *Mol Cell Biol* 1994;14:5192–5201.
4. Giorgetti S, Pelicci PG, Pelicci G, Van Obberghen E. Involvement of Src-homology/collagen (SHC) proteins in signaling through the insulin receptor and the insulin-like-growth-factor-I-receptor. *Eur J Biochem* 1994;223:195–202.
5. Sadoshima J, Izumo S. The heterotrimeric G q protein-coupled angiotensin II receptor activates p21 ras via the tyrosine kinase-Shc-Grb2-Sos pathway in cardiac myocytes. *EMBO J* 1996;15:775–787.
6. Chen KD, Li YS, Kim M, Li S, Yuan S, Chien S, Shyy JY. Mechanotransduction in response to shear stress: roles of receptor tyrosine kinases, integrins, and Shc. *J Biol Chem* 1999;274:18393–18400.
7. Migliaccio E, Giorgio M, Mele S, Pelicci G, Reboldi P, Pandolfi PP, Lanfrancone L, Pelicci PG. The p66Shc protein controls oxidative stress response and life span in mammals. *Nature* 1999;402:309–313.
8. Lee MK, Zhao J, Smith S, Tefft JD, Bringas P Jr, Hwang C, Warburton D. The Shc 66 and 46 kDa isoforms are differentially downregulated at parturition in the fetal mouse lung. *Pediatr Res* 1998;44:850–859.
9. Northway WH Jr, Rosan RC, Porter DY. Pulmonary disease following respirator therapy of hyaline-membrane disease: bronchopulmonary dysplasia. *N Engl J Med* 1967;276:357–368.
10. Coalson JJ, Winter VT, Siler-Khodr T, Yoder BA. Neonatal chronic lung disease in extremely immature baboons. *Am J Respir Crit Care Med* 1999;160:1333–1346.
11. Sunday ME, Yoder BA, Cuttitta F, Haley KJ, Emanuel RL. Bombesin-like peptide mediates lung injury in a baboon model of bronchopulmonary dysplasia. *J Clin Invest* 1998;102:584–594.
12. Coalson JJ. Pathology of new bronchopulmonary dysplasia. *Semin Neonatol* 2003;8:73–81.
13. Lee MK, Smith SM. p66Shc expression is differentially regulated in fetal lung development and chronic lung disease [abstract]. *Am J Respir Crit Care Med* 2002;165:A645.
14. Coalson JJ, Winter VT, Siler-Khodr T, Yoder BA. Neonatal chronic lung disease in extremely immature baboons. *Am J Respir Crit Care Med* 1999;160:1333–1346.
15. Escobedo MB, Hilliard JL, Smith F, Meredith K, Walsh W, Johnson D, Coalson JJ, Kuehl TJ, Null DM Jr, Robotham JL. A baboon model of bronchopulmonary dysplasia: I. Clinical features. *Exp Mol Pathol* 1982;37:323–334.
16. Kleinbaum DG, Kupper LL, Muller KE. Two-way ANOVA with equal cell numbers. In: Applied regression analysis and other multivariate methods, 2nd ed. Boston, MA: PWS-Kent; 1988. pp. 416–456.
17. Rosner B. Hypothesis testing: two-sample inference. In: Fundamentals of biostatistics, 3rd ed. Boston, MA: PWS-Kent; 1990. pp. 248–292.
18. Celis JE, Celis A. Cell cycle-dependent variations in the distribution of the nuclear protein cyclin proliferating cell nuclear antigen in cultured cells: subdivision of S phase. *Proc Natl Acad Sci USA* 1985;82:3262–3266.
19. Oliver FJ, de la Rubia G, Rolli V, Ruiz-Ruiz MC, de Murcia G, Murcia JM. Importance of poly(ADP-ribose) polymerase and its cleavage in apoptosis: lesson from an uncleavable mutant. *J Biol Chem* 1998;273:33533–33539.
20. Yang CP, Horwitz SB. Distinct mechanisms of taxol-induced serine phosphorylation of the 66-kDa Shc isoform in A549 and RAW 264.7 cells. *Biochim Biophys Acta* 2002;1590:76–83.
21. Lotti LV, Lanfrancone L, Migliaccio E, Zompetta C, Pelicci G, Salcini AE, Falini B, Pelicci PG, Torrisi MR. Shc proteins are localized on endoplasmic reticulum membranes and are redistributed after tyrosine kinase receptor activation. *Mol Cell Biol* 1996;16:1946–1954.
22. Smith CI, Searls RL, Hilfer SR. Effects of hormones on functional differentiation of mouse respiratory epithelium. *Exp Lung Res* 1990;16:191–209.
23. DiFiore JW, Wilson JM. Lung development. *Semin Pediatr Surg* 1994;3:221–232.
24. Toti P, Buonocore G, Tanganelli P, Catella AM, Palmeri ML, Vatti R, Seemayer TA. Bronchopulmonary dysplasia of the premature baby: an immunohistochemical study. *Pediatr Pulmonol* 1997;24:22–28.
25. Okada S, Kao AW, Ceresa BP, Blaikie P, Margolis B, Pessin JE. The 66-kDa Shc isoform is a negative regulator of the epidermal growth factor-stimulated mitogen-activated protein kinase pathway. *J Biol Chem* 1997;272:28042–28049.
26. Maniscalco WM, Watkins RH, O'Reilly MA, Shea CP. Increased epithelial cell proliferation in very premature baboons with chronic lung disease. *Am J Physiol Lung Cell Mol Physiol* 2002;283:L991–L1001.
27. Trinei M, Giorgio M, Cicalese A, Barozzi S, Ventura A, Migliaccio E, Milia E, Padura IM, Raker VA, Maccarana M, *et al.* A p53-p66Shc signalling pathway controls intracellular redox status, levels of oxidation-damaged DNA and oxidative stress-induced apoptosis. *Oncogene* 2002;21:3872–3878.
28. Pacini S, Pellegrini M, Migliaccio E, Patrussi L, Ulivieri C, Ventura A, Carraro F, Naldini A, Lanfrancone L, Pelicci P, *et al.* p66SHC promotes apoptosis and antagonizes mitogenic signaling in T cells. *Mol Cell Biol* 2004;24:1747–1757.
29. Gotoh N, Toyoda M, Shibuya M. Tyrosine phosphorylation sites at amino acids 239 and 240 of Shc are involved in epidermal growth factor-induced mitogenic signaling that is distinct from Ras/mitogen-activated protein kinase activation. *Mol Cell Biol* 1997;17:1824–1831.
30. Klint P, Kanda S, Claesson Welsh L. Shc and a novel 89-kDa component couple to the Grb2-Sos complex in fibroblast growth factor-2-stimulated cells. *J Biol Chem* 1995;270:23337–23344.